THE JOURNAL OF PHYSICAL CHEMISTRY B



B: Biophysics; Physical Chemistry of Biological Systems and Biomolecules

# Kaempferol Binding to zinc(II). Efficient Radical Scavenging through Increased Phenol Acidity

Yi Xu, Lingling Qian, Jing Yang, Rui-Min Han, Jian-Ping Zhang, and Leif H. Skibsted

*J. Phys. Chem. B*, **Just Accepted Manuscript** • DOI: 10.1021/acs.jpcb.8b08284 • Publication Date (Web): 08 Oct 2018



ACS Publications

is published by the American Chemical Society. 1155 Sixteenth Street N.W., Washington, DC 20036

# Kaempferol Binding to Zinc(II). Efficient Radical Scavenging Through Increased Phenol Acidity

*Yi Xu*[†], *Ling-Ling Qian*[†], *Jing Yang*[†], *Rui-Min Han*[†]*, *Jian-Ping Zhang*[†], *Leif H. Skibsted*[‡]*

[†]Department of Chemistry, Renmin University of China, Beijing, 100872

[‡]Department of Food Science, University of Copenhagen, Rolighedsvej 30, DK-1058 Frederiksberg C, Denmark

E-mail addresses of authors：

Rui-Min Han: rmhan@ruc.edu.cn

Yi Xu: yixu@ruc.edu.cn

Ling-Ling Qian: qianlingling@ruc.edu.cn

Jing Yang: yangjing2015@ruc.edu.cn

Jian-Ping Zhang: jpzhang@ruc.edu.cn

Leif H. Skibsted: ls@food.ku.dk

*Corresponding author

Ph. D. Rui-Min Han

Tel: +86-10-6251-6604; Fax: +86-10-6251-6444

E-mail: rmhan@ruc.edu.cn

and

Professor Leif H. Skibsted

Tel: +45-3533-3221

E-mail: ls@food.ku.dk

**ABSTRACT:** Zinc(II) enhances radical scavenging of the flavonoid kaempferol (Kaem) most significantly for the 1:1 Zn(II)-kaempferol complex in equilibrium with the 1:2 Zn(II)-kaempferol complex both with high-affinity at 3-hydroxyl and 4-carboxyl coordination. In methanol/chloroform (7/3, v/v), 1:1 Zn(II)-kaempferol complex reduces $\beta$-carotene radical cation, $\beta$-Car$^{\bullet+}$, with a second-order rate constant, $1.88\times10^{8}$ L·mol$^{-1}$·s$^{-1}$, while both Kaem and 1:2 Zn(II)-kaempferol complex are non-reactive, as determined by laser flash photolysis. In ethanol, 1:1 Zn(II)-kaempferol complex reduces the 2,2-diphenyl-1-picrylhydrazyl radical, DPPH$^{\bullet}$, with a second order rate constant, $2.48\times10^{4}$ L·mol$^{-1}$·s$^{-1}$, 16 times and 2 times as efficient as Kaem and 1:2 Zn(II)-kaempferol complex, respectively, as determined by stopped-flow spectroscopy. Density functional theory (DFT) calculation results indicate significantly increased acidity of Kaem as ligand in 1:1 Zn(II)-kaempferol complex other than in 1:2 Zn(II)-kaempferol complex. Kaem in 1:1 Zn(II)-kaempferol complex loses two protons (one from 3-hydroxyl and one from phenolic hydroxyl) forming 1:1 Zn(II)-(Kaem−2H) during binding with Zn(II), while Kaem in 1:2 Zn(II)-kaempferol complex loses one proton in each ligand forming Zn(II)-(Kaem–H)$_2$, as confirmed by UV-vis absorption spectroscopy. Zn(II)-(Kaem−2H) is a far stronger reductant than Kaem and Zn(II)-(Kaem−H)$_2$ as determined by cyclic voltammetry. Significant rate increases for the 1:1 complex in both $\beta$-Car$^{\bullet+}$ scavenging by electron transfer (ET) and DPPH$^{\bullet}$ scavenging by hydrogen atom transfer (HAT) were ascribed to decreases of ionization potential (IP) and of bond dissociation energy (BDE) of 4´-OH for deprotonated Zn(II)-(Kaem−2H), respectively. Increased phenol acidity of plant polyphenols by 1:1 coordination with Zn(II) may explain the unique function of Zn(II) as a biological antioxidant and may help to design non-toxic metal-based drugs derived from natural bioactive molecules.

## 1. INTRODUCTION

Zinc, as an important micronutrient, is a cofactor for more than 300 metalloenzymes essential for growth and development of nearly all organisms.[1-4] Zn(II) is crucial for the function of superoxide dismutase through structural support for the Cu(I)/Cu(II) cycling.[5] Zinc has also been found to improve resistance to oxidative stress as an antioxidant despite that Zn(II) is the only oxidation state of importance for zinc in biological systems.[6-10] Zinc biofortification recently was also found improving nutritional quality and antioxidant system of green bean grown under greenhouse conditions.[11] Otherwise the antioxidative activity of Zn(II) based on molecular level is poorly understood.

Flavonoids, as secondary plant metabolites of polyphenols family, have important biological activities such as antioxidant, anti-inflammatory, and anticancer.[12,13] Kaempferol (Kaem, Scheme 1a) found in a variety of plants and plant-derived common foods, contributes approximately ~4 mg/day in the total average intake of flavonoid in a normal diet.[14] Kaem has been reported to have important biological functions as metal chelators and radical scavengers.[15-16] Notably, most metal chelates of flavonoids have often been found to be better antioxidants and to have more significant biological effects than their parent flavonoids.[17-28] Such enhancement in antioxidative activity of flavonoid complexes may be understood for transition metal ions like copper(II) and iron(III) as a result of the reduction of central metal ions.[17, 29-31]

Zn(II) has, however, been found to coordinate flavonoids and other biomolecules, which may affect the transport and uptake of zinc,[32] and also alter the radical scavenging properties of such plant polyphenols.[9,33-36] Zn(II) complexes of Kaem, have recently been found to have anticancer activity.[10]For the redox-inert metal zinc, different from copper and iron containing different oxidation states, other mechanisms must be operating, but have not been identified or studied in any details despite a growing interest in medical application of Zn(II) coordination compounds. Zinc, as a non-toxic metal, often

becomes the first choice as a carrier or modifier of biological active secondary plant metabolites like the flavonoids in the development of new metal-based drugs.[33]

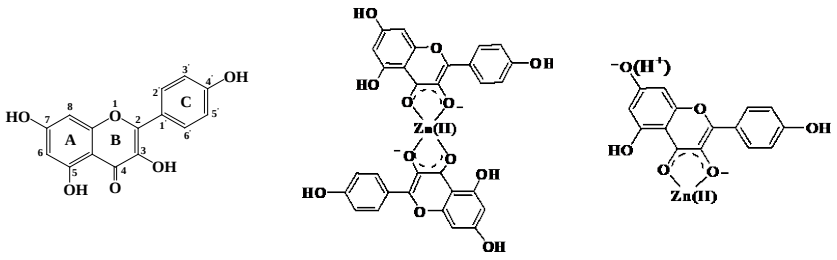


**(a)** **(b)** **(c)**

**Scheme 1.** Molecular structures of (a) kaempferol (Kaem), and complexes of Kaem with Zn(II) ion, (b) 1:2 Zn(II)-$(Kaem–H)_2$ and (c) 1:1 Zn(II)-$(Kaem–H)^+$ and deprotonated Zn(II)-(Kaem–2H), with and without 7-phenolic proton, as the most acidic group based on the following DFT calculations.

Reported are results from a study of Zn(II) complexes of Kaem combining spectroscopy for structural characterization with results from investigations of reaction dynamics of the Zn(II) complexes with radicals. Reactions with the very reactive *β*-carotene radical cation, *β*-$Car^{\bullet+}$, and with the semi-stable 1,1-diphenyl-2-picrylhydrazyl radical, $DPPH^{\bullet}$, show common features for Kaem complexes despite the different time regime for their reactions. The results point toward a more general mechanism for zinc as an antioxidant entailing coupling with proton dissociation of plant polyphenols.

## 2. EXPERIMNENTAL SECTION

**2.1 Chemicals.** Kaempferol (Kaem, >98%) and apigenin (Api, >98%) from Huike Plant Exploitation Inc, (Shanxi, China), zinc acetate dihydrate ($Zn(CH_3COO)_2 \cdot 2H_2O$, >99%), from Beijing Chemical Reagents Company, China, acetic acid ($CH_3COOH$, >99.5%) from Titan Scientific,(Shanghai, China), 1,1-diphenyl-2-picrylhydrazyl radical ($DPPH^{\bullet}$) from ZhongShengRuiTai Technology Inc (>97%, Beijing, China) were used as received. All-*trans*-*β*-carotene (*β*-Car, >93%), ferrocene (>98%), $NaClO_4$ (>98%), methanol-d4 (>99.8%) and chloroform-d (>99.8%) from Sigma-Aldrich (St. Louis, MO, USA) were used as received. Spectrophotometric grade methanol and ethanol (99.9%, Fine Chemical Industry Research

Institute, Tianjin, China) were used as received. Chloroform (>99.0%, Beijing Chemical Works, Beijing, China) was purified before use by passing through an alumina column (AR, Tianjin Fuchen Chemical Plant, Tianjin, China).

**2.2 Reaction of Zn(II) with Kaempferol.** All UV-vis absorption spectra were measured on a Cary50 spectrophotometer (Varian, Inc., Palo Alto, CA, USA) using 1.0 cm quartz cells in a thermostated room at 25°C. The solutions were prepared by mixing solutions of Kaem and $Zn(CH_3COO)_2$ with total molar concentrations of $5.0\times10^{-5}$ M in Kaem/Zn(II) molar ratios varying from 19:1 to 1:19.

**2.3 IR, NMR and Mass Spectra.** IR spectra were obtained on Bruker Tensor 27 FT-IR spectrometer (Karlsruke, Germany). Solid samples of Zn(II)-kaempferol complexes for IR tableting were prepared from a solutions of Kaem and $Zn(CH_3COO)_2$ in ratios of 1:1 and 1:2 by evaporation of ethanol with a nitrogen gas flow.

$^1$H-NMR spectra were obtained on a Bruker AM 400 MHz spectrometer (Karlsruhe, Germany). Sample of Zn(II)-kaempferol complexes for $^1$H-NMR determination were prepared by dissolving the solid sample as obtained for IR spectra in deuterated methanol and chloroform.

MS spectra were obtained on a Thermo Scientific™ Q Exactive™ HF (Waltham, MA, USA) in the positive ion mode. Sample of Zn(II)-kaempferol complexes were prepared by filtering solutions of Kaem and $Zn(CH_3COO)_2$ after mixing through a nylon membrane with 220 nm sieve pores. The samples were analyzed by direct infusion ESI by means of a syringe pump (Thermo UltiMate 3000,Waltham, MA, USA) at a flow rate of 5 μL/min. Capillary temperature was 320°C and spray voltage was 3.50 kV.

**2.4 *β*-Carotene Radical Cation and DPPH$^{\bullet}$ Scavenging.** The laser flash photolysis apparatus for the study of the kinetics of $\beta$-Car$^{\bullet+}$ scavenging has previously been described in detail.[37,38] The laser pulses at 532 nm (4 mJ/pulse, 7 ns, and 10 Hz) for the bleaching assay were supplied by a $Nd^{3+}$: YAG laser (Quanta-Ray PRO-230, Spectra Physics Lasers, Inc., Mountain View, CA, USA). 940 and 510 nm probe

lights were provided by a laser-driven white light source (LDLS-EQ-99 LAMP MODULE, Energetiq Technology, Inc., Woburn, MA). The absorbance was detected with a photodiode (model S3071, Hamamatsu Photonics, Hamamatsu, Japan). The optical path length of the flow cuvette was 1 cm. All of the measurements were carried out in a thermostated room of 25 °C. Methanol/chloroform (7/3, v/v) was used as the solvent for the equilibrated solution of $\beta$-Car and $Zn(CH_3COO)_2$ and Kaem.

The kinetics of DPPH$^{\bullet}$ scavenging by Zn(II)-kaempferol complexes was investigated by using a rapid mixing, stopped-flow technique using the same method as previously, performed on RX2000 Rapid-Mixing Stopped-Flow Unit (Applied Photophysics Ltd, Surrey, United Kingdom). For one syringe solution, DPPH$^{\bullet}$ was dissolved in ethanol to obtain an absorbance of 0.92±0.02 (extinction coefficient $\varepsilon$ = 9660 $L \cdot mol^{-1} \cdot cm^{-1}$) at 516 nm, the final concentration of the DPPH$^{\bullet}$ was calculated to be 100 μM. The other syringe solution was an equilibrated solution of $Zn(CH_3COO)_2$ and Kaem.

**2.5 Determination of Oxidation Potentials.** Cyclic voltammetry (CV) was performed on a three-electrode CHI 760D electrochemical analyzer (ChenHua Instruments Inc., Shanghai, China). The working electrode was a glassy carbon piece (diameter=4 mm), the reference electrode was a silver wire, and the auxiliary electrode was a platinum wire. 0.10 M $NaClO_4$ was used as supporting electrolyte. $5.0\times10^{-5}$ M ferrocene was used as internal standard, and CVs were obtained in the potential range of –0.4 V to 0.6 V at 0.1 V/s scan rate.

**2.6 Quantum Chemical Calculations.** Structural optimizations, calculation of electronic density and bond lengths of Kaem and three Zn(II)-kaempferol complexes were performed using the Gaussian 09 package with the Becke3 and Lee Yang Parr (B3LYP) hybrid functional method.[39] The 6-31+G(d) basis set and the LANL2DZ pseudopotential, were chosen for C, O, and H atoms, and for the Zn(II) cation, respectively.

The proton dissociation enthalpy (PDE), ionization potential (IP) and bond dissociation enthalpy (BDE) of both Kaem and Zn(II)-kaempferol complexes were calculated as gas phase enthalpy difference:

$$\text{Ar-OH} \rightarrow \text{Ar-O}^{\bullet} + \text{H}^{\bullet}$$

$$\text{Ar-OH} \rightarrow \text{Ar-O}^{-} + \text{H}^{+}$$

$$\text{Ar-OH} \rightarrow \text{Ar-OH}^{\bullet+} + e$$

$$\text{Ar-O}^{-} \rightarrow \text{Ar-O}^{\bullet} + e$$

Ar represents an unsaturated group linked to hydroxyl in Kaem or Zn(II)-kaempferol complexes. Enthalpies of $H^{\bullet}$ ($-312.64$ kcal·mol$^{-1}$) and $H^{+}$ (1.48 kcal·mol$^{-1}$) were also calculated and the enthalpy of electron (0.75 kcal·mol$^{-1}$) was obtained from literature.[40]

## 3. RESULTS

**3.1 Formation and Characterization of Two Zn(II)-Kaempferol Complexes.** $Zn(CH_3COO)_2$ red-shifts the UV-visible absorption spectrum of kaempferol (Kaem) as seen in Figure 1a for Kaem dissolved in ethanol together with $Zn(CH_3COO)_2$ in a Kaem/Zn(II) ratio varying from 19:1 to 1:19. The spectral changes indicate binding of Zn(II) to Kaem in a stepwise manner with an initial broadening of the Kaem spectrum for increasing Zn(II) addition followed by appearance of a new absorption band at 440 nm. The spectral changes are indicative of formation of two species, Zn(II)-Kaem$_p$ complex dominating for Kaem in excess as equilibrium of equation (1) and Zn(II)-Kaem$_q$ complex dominating for increasing Zn(II) in excess as equilibrium of equation (2):

$$\text{Zn(II)} + p\text{Kaem}(ex) \overset{-p\text{H}^{+}}{\rightleftharpoons} \text{Zn(II)-Kaem}_p \qquad (1)$$

$$\text{Zn(II)}(ex) + q\text{Kaem} \overset{-q\text{H}^{+}}{\rightleftharpoons} \text{Zn(II)-Kaem}_q \qquad (2)$$

in which $p > q > 0$, where both $p$ and $q$ may be integers or decimal numbers.

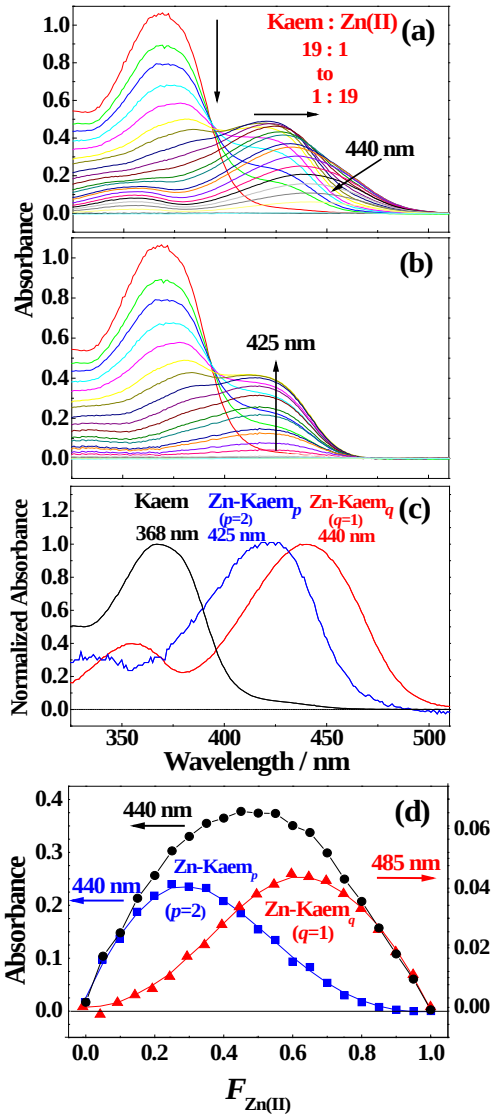


**Figure 1**. (a) Absorption spectra of Kaem and $Zn(CH_3COO)_2$ in a total concentration 50 μM in different ratios varying from 19:1 to 1:19 in ethanol. (b) Absorption difference spectra of all spectra in Figure 1a subtracting spectra of Zn-Kaem$_q$($q$=1). Detailed description was presented in text. (c) Normalized absorption spectra of Kaem and deconvoluted spectra of Zn(II)-Kaem$_p$ ($p$=2) and Zn(II)-Kaem$_q$ ($q$=1). (d) Job's-Plots of spectra in Figure 1a at 440 nm and deconvoluted absorbances of Zn-Kaem$_p$ ($p$=2) at 440 nm and Zn-Kaem$_q$ ($q$=1) at 485 nm against molar fractions of zinc ion, $F_{Zn(II)}$.

The absorption spectrum of Zn(II)-Kaem$_q$ obtained from normalized spectra (*for condition where changes were not seen for further addition of Zn(II)* ) with zinc (II) in excess as seen in Figure 1a. A series of difference spectra excluding Zn(II)-Kaem$_q$ as component but with contribution from Zn(II)-Kaem$_p$ and Kaem are shown in Figure 1b after subtraction the calculated Zn(II)-Kaem$_q$ spectrum from the original spectra using equation:

$$S = S_0 - S_{\text{Zn(II)- Kaem}_q} \times \frac{A_{0\_485nm}}{A_{\text{Zn(II)- Kaem}_q\_485nm}} \quad (3)$$

in which, $S$, $S_0$ *and* $S_{\text{Zn(II)- Kaem}_q}$ represent spectra after (Figure 1b) and before (Figure 1a) subtracting the Zn(II)-Kaem$_q$ component, and spectrum of Zn(II)-Kaem$_q$ (Figure 1c), respectively. $A_{0\_485nm}$ and $A_{\text{Zn(II)-Kaem}_q\_485nm}$ represent absorbances at 485 nm for original spectra before subtracting the spectrum of Zn(II)-Kaem$_q$ and the spectrum of Zn(II)-Kaem$_q$, respectively.

The absorption spectrum of Zn(II)-Kaem$_p$ obtained using the same method as for Zn(II)-Kaem$_q$ is shown in Figure 1c together with spectra of Zn(II)-Kaem$_q$ and Kaem. The Job's-Plots[41] for 440 nm based on spectra in Figure 1a and the independent contribution to absorbance for Zn(II)-Kaem$_p$ at 440 nm and Zn(II)-Kaem$_q$ at 485 nm as a function of the molar fraction of Zn(II) are shown in Figure 1d.

Using the numerical methods in reference,[42] $p$ = 2 and $q$ = 1 were resolved using equations (S12) and (S13) in Supporting Information. Equations (1) and (2) may accordingly be written as new forms:

$$\text{Zn(II)} + \text{Kaem} \overset{-\text{H}^+, K_1}{\rightleftharpoons} \text{Zn(II)-Kaem} \quad (4)$$

$$\text{Zn(II)-Kaem} + \text{Kaem} \overset{-\text{H}^+, K_2}{\rightleftharpoons} \text{Zn(II)-Kaem}_2 \quad (5)$$

Formation constants in equations (4) and (5) are calculated to have values $K_1 = 4.8\times10^5$ L·mol$^{-1}$ for Zn(II)-Kaem and $K_2 = 2.5\times10^5$ L·mol$^{-1}$ for Zn-Kaem$_2$, respectively (see Supporting Information). A similar analyses based on Jobs method for equilibrium spectra of Kaem and Zn(CH$_3$COO)$_2$ in methanol:chloroform (7/3, v/v) gave the stability constants $K_1$=1.0×10$^5$ L·mol$^{-1}$ for Zn(II)-Kaem and $K_2$=2.0×10$^5$ L·mol$^{-1}$ for Zn-Kaem$_2$. Equilibrium fractions of Kaem and two complexes for the concentration ratios used for the structural characterization and for radical scavenging dynamics in ethanol and methanol:chloroform (7/3, v/v) are shown in Table 1.

The spectral changes for Zinc(II) reaction with Kaem are different from Zn(II)-apigenin complex with chelation occurring at 4-carbonyl and 5-hydroxyl (Figure S2), but similar ~50 nm spectral red shift compared to parent flavonoids was observed for 1:2 Zn(II)-Kaem$_2$ and Zn(II)-3-hydroxyflavone

complex.[43] Chelating site in Zn(II)-kaempferol complexes is accordingly ascribed to 3-hydroxyl and 4-carbonyl groups. The remaining isolated 5-, 7- or 4´-hydroxyls can not associated with metal chelation[10]

**Table 1.** Fractions (*F*, %) of Kaem, Zn(II)-(Kaem–H)$_2$ and Zn(II)-(Kaem–2H) in ethanol and in methanol:chloroform (7/3) at indicated varying ratios.

| Kaem: Zn(II) | ethanol / methanol:chloroform(7:3) | | |
|---|---|---|---|
| | $F_{Kaem}$(%) | $F_{Zn(II)-(Kaem-H)2}$(%) | $F_{Zn(II)-(Kaem-2H)}$(%) |
| 1:0 | 100/100 | 0/0 | 0/0 |
| 1:0.2 | 61.3/61.9 | 37.6/36.6 | 1.1 / 1.5 |
| 1:0.5 | 13.8/19.2 | 75.7/71.4 | 10.5/9.4 |
| 1:1 | 2.7/6.5 | 57.1/67.4 | 40.2/26.1 |
| 1:2 | 1.1/3.3 | 36.3/54.4 | 62.6/42.3 |
| 1:5 | 0.4/1.5 | 18.0/36.4 | 81.6/62.1 |
| 1:10 | 0.2/0.7 | 9.9/24.4 | 89.9/74.9 |
| 1:20 | 0.1/0.4 | 5.2/15.0 | 94.7/84.6 |

Solutions: 100 µM Kaem with 0, 20, 50, 100, 200, 500, 1000, 2000 µM Zn(CH3COO)2, respectively.Zn(II)-(Kaem–H)$_2$ and Zn(II)-(Kaem–2H) are the specific forms of 1:2 Zn-Kaem$_2$ and 1:1 Zn-Kaem, respectively, and will be further explained in the following..

The 15 nm red-shift of the absorption of Zn(II)-Kaem compared to Zn(II)-Kaem$_2$ in Figure 1c is indicative of phenolic deprotonation in Zn(II)-Kaem as confirmed by acid sensitivity of the visible spectrum of Zn(II)-Kaem. Zn(II)-Kaem was found to transform into Zn(II)-Kaem$_2$ with the spectral red-shift reversed, by addition of acetic acid see Figure 2.

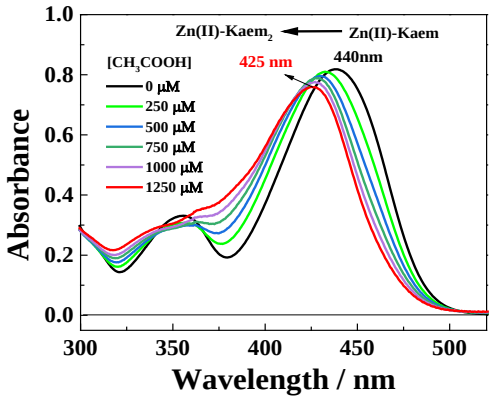


**Figure 2.** Absorption spectra changes of 50 µM Kaem in the presence of 500 µM Zn(CH$_3$COO)$_2$ with addition of 250, 500, 750, 1000 and 1250 µM CH$_3$COOH.

Formation of 1:2 complex involves loss of a proton from 3-hydroxyl of each Kaem ligand when binding with zinc thus written as **Zn(II)-(Kaem–H)$_2$** (Scheme 1b), similar to reported 1:2 Cu(II)-quercetin and Zn(II)/Mg(II)-primuletin complexes:[44,45]

$$Zn(II) + 2Kaem \overset{-2H^+}{\rightleftharpoons} Zn(II)\text{-}(Kaem-H)_2 \quad (6)$$

While, formation of 1:1 complex involves loss of one proton from 3-hydroxyl of Kaem generates a cationic form, **Zn(II)-(Kaem–H)$^+$** (with 7-phenolic proton in Scheme 1c).[10,46] A second proton from 7-phenolic hydroxyl (*the most acidic group among three unchelated phenolic hydroxyls, will be further explained based on the following DFT calculations*) is lost from the same Kaem ligand eventually forming **Zn(II)-(Kaem–2H)** (without 7-phenolic proton in Scheme 1c):

$$Zn(II) + Kaem \overset{-H^+}{\rightleftharpoons} Zn(II)\text{-}(Kaem-H)^+ \overset{-H^+}{\rightleftharpoons} Zn(II)\text{-}(Kaem-2H) \quad (7)$$

The equilibrium transformation between two complexes, 1:1 Zn(II)-(Kaem–2H) and 1:2 Zn(II)-(Kaem–H)$_2$, depends on concentrations of hydrogen ion and Zn(II) ion (Scheme 2):

$$2Zn(II)\text{-}(Kaem-2H)+2H^+ \rightleftharpoons Zn(II)\text{-}(Kaem-H)_2+Zn(II) \quad (8)$$

Accordingly, Zn(II)-(Kaem–H)$^+$ and Zn(II)-(Kaem–2H) are used for representing 1:1 Zn(II)-Kaem before and after second deprotonation, respectively, and Zn(II)-(Kaem–H)$_2$ for 1:2 Zn(II)-Kaem$_2$ in the following texts.

IR spectrum data of Zn(II)-kaempferol complexes in Table SI further support above assignment of Kaem binding to Zn(II) with 3-hydroxyl and 4-carbonyl groups. Mass spectrometry and $^1$H-NMR spectroscopy (Figures S3, S4 and Tables S2, S3) confirmed the composition of Zn(II)-(Kaem−H)$_2$ and Zn(II)-(Kaem−2H) as obtained by Jobs method of continuous variation using Uv-visible spectra. (see Supporting Information)

**3.2 Determinations of Oxidation Potentials.** Kaem was found to be oxidized by a quasi-reversible process using cyclic voltammetry and has an oxidation potential of 0.179 V versus ferrocene from the CV scan of 100 μM Kaem and Zn(II) for ratios varying from 5:1 to 1:20 as shown in Figure 3a and Table2.

Oxidation potentials are obtained from initial oxidation peak corresponding to oxidation of phenolic group.[47,48] The significant decrease in oxidation potential from 0.179 V to −0.097 V by increasing addition of Zn(II) ion agrees well with the increase of the Zn(II)-(Kaem−2H) percentage as shown in Figure 3b. Kaem and 1:2 Zn(II)-(Kaem−H)$_2$ are found to have very similar oxidation potential, ~0.170 V, while Zn(II)-(Kaem−2H) is far more reducing with an oxidative potentials, approximately −0.097 V, obtained from sample of Kaem and Zn(II) in ratio of 1:20. Such remarkable decreases in oxidation potentials were also observed for complexes of Zn(II), Al(III) and Eu(III) with quercetin, rutin and galangin.[35,49]

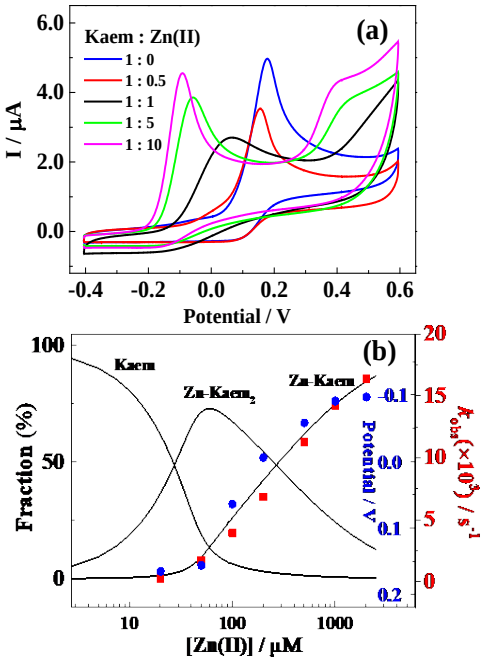


**Figure 3**. (a) Cyclic voltammograms of 100 μM Kaem and solutions of 100 μM Kaem with 20, 50, 100, 200, 500 and 1000 μM $Zn(CH_3COO)_2$ in relative to 50 μM ferrocene and 0.1 M $NaClO_4$. (b) Oxidation potentials obtained from Figure 3a (*blue circle*), observed first order rate constants obtained from single exponential fitting the decay of $\beta$-Car$^{\bullet+}$ at 940 nm in Figure 4a (*red square*), and molar fractions (*solid lines*) of Kaem and deconvoluted Zn(II)-(Kaem−H)2 and Zn(II)-(Kaem−2H) against concentration of $Zn(CH_3COO)_2$ calculated from formation constants, $K_1$=1.0×10$^5$ L·mol$^{-1}$ and $K_2$=2.0×10$^5$ L·mol$^{-1}$. Solvent is methanol / chloroform (7/3, v/v).

**3.3 Radical Scavenging Kinetics.** Antioxidant activities of Kaem and complexes of Zn(II) with Kaem were evaluated using two radical scavenging methods: (i) scavenging of the photo-induced carotenoid radical cations $\beta$-Car$^{\bullet+}$ in methanol/chloroform (7/3, v/v), and (ii) scavenging of the semi-stable radical DPPH$^{\bullet}$ in ethanol.

**3.3.1 $\beta$-Car$^{\bullet+}$ Radical Scavenging Kinetics.** Bleaching of $\beta$-Car in methanol/chloroform to generate $\beta$-Car$^{\bullet+}$ using laser flash photolysis and time resolved absorption spectroscopy were previously established for comparison of the antioxidant activity of polyphenols.[37,38] The decay of $\beta$-Car$^{\bullet+}$ absorbing at 940 nm is not affected by the presence of Zn(II) or Kaem alone, or even Kaem and Zn(II) with ratio at 1:0.2, but is increasingly accelerated by addition of Zn(II) to Kaem solutions at varying Zn(II):Kaem ratios from 1:0.5 to 1:20 as seen in Figure 4a.

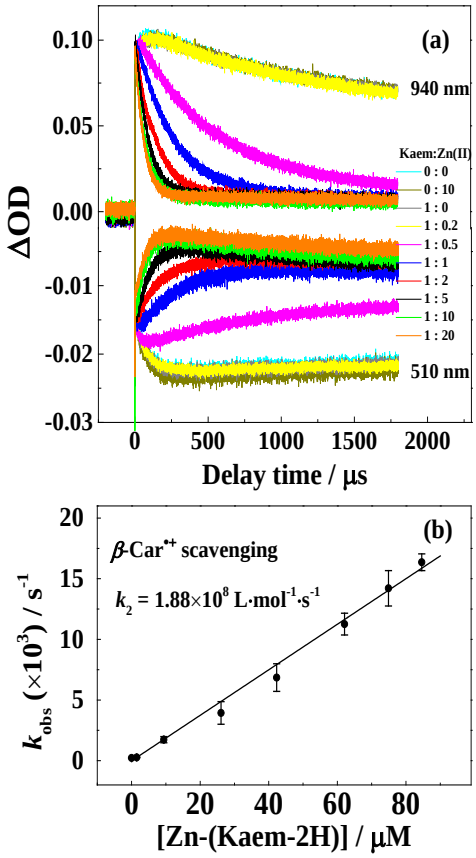


**Figure 4.** (a) Decay of $\beta$-Car$^{\bullet+}$ as monitored at 940 nm and bleaching recovery of $\beta$-carotene ground state as absorbance at 520 nm in the absence and presence of 100 μM Kaem, of 100 μM $Zn(CH_3COO)_2$, and of 100 μM Kaem with 20, 50, 100, 200, 500, 1000 and 2000 μM $Zn(CH_3COO)_2$, respectively. (b) Observed first order rate constants obtained from single exponential fitting the decay of $\beta$-Car$^{\bullet+}$ in Figure 4a against concentration of $Zn(CH_3COO)_2$. Second-order rate constant is calculated to be $k_2$=1.88±0.05×10$^8$ L·mol$^{-1}$·s$^{-1}$. All in methanol/chloroform (7/3) at 25°C.

The recovery of $\beta$-Car bleaching at 510 nm is similarly as kinetics at 940 nm, not affected by presence of Zn(II) or Kaem alone, or solution of Kaem:Zn(II)=1:0.2, but is significantly accelerated by increasing addition of Zn(II) to Kaem.

Absorbance decay at 940 nm could be accommodated by a single exponential function, and the observed rate constants, $k_{Car^{\bullet+}}$ listed in Table 2, are found in good agreement with the increase of the fraction of Zn(II)-(Kaem−2H) present and with the decrease in the oxidation potential of the equilibrium mixture as shown in Figure 3b. Linear dependence of $k_{Car^{\bullet+}}$ on the concentration of Zn(II)-(Kaem−2H) (Figure 4b), implicates that Zn(II)-(Kaem-2H) complex is the only $\beta$-Car$^{\bullet+}$ radical scavenger with very low oxidation potential −0.097 V. Kaem and 1:2 Zn(II)-(Kaem-H)$_2$ are non-reactive in $\beta$-Car$^{\bullet+}$ scavenging due to their higher oxidation potential ~0.170 V than −0.097 V for Zn(II)-(Kaem-2H).

Simultaneous increase in rates of $\beta$-Car$^{\bullet+}$decay at 940 nm and of bleaching recovery at 510 nm confirm electron transfer from Zn(II)-(Kaem-2H) to $\beta$-Car$^{\bullet+}$, i.e. $\beta$-Car$^{\bullet+}$ was reduced and regenerated to $\beta$-Car by Zn(II)-(Kaem-2H):

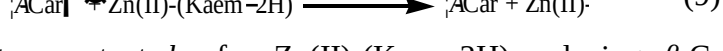

$$\beta\text{-Car}^{\bullet+} + \text{Zn(II)-(Kaem}-2\text{H)} \xrightarrow{k_2^{\text{Zn(II)-(Kaem-2H)}}} \beta\text{-Car} + \text{Zn(II)}^{\bullet} \qquad (9)$$

The second-order rate constant $k_2$ for Zn(II)-(Kaem-2H) reducing $\beta$-Car$^{\bullet+}$ is obtained to be $(1.88\pm0.05)\times10^8$ L·mol$^{-1}$·s$^{-1}$ based on the linear relationship in Figure 4b.

**Table 2.** Observed first order rate constants for the decay of $\beta$-Car$^{\bullet+}$ ($k_{Car^{\bullet+}}$, $s^{-1}$) and of DPPH$^{\bullet}$ ($k_{DPPH^{\bullet}}$, $s^{-1}$), and oxidation potentials determined by CV at indicated varying ratios.

| Kaem:Zn(II) | $k_{Car^{\bullet+}}$ ($s^{-1}$) | $k_{DPPH^{\bullet}}$ ($s^{-1}$) | Potential (V) |
|---|---|---|---|
| **1:0** | **$2.2\pm0.1\times10^2$** | **0.15±0.01** | **0.179** |
| **1:0.2** | **2.7±0.2×102** | **---** | **0.165** |
| **1:0.5** | **$1.7\pm0.2\times10^3$** | **0.67±0.01** | **0.156** |
| **1:1** | **$3.9\pm1.0\times10^3$** | **1.19±0.03** | **0.064** |
| **1:2** | **$6.9\pm1.1\times10^3$** | **1.79±0.08** | **−0.006** |
| **1:5** | **$1.1\pm0.1\times10^4$** | **---** | **−0.058** |
| **1:10** | **$1.4\pm0.1\times10^4$** | **1.99±0.07** | **−0.091** |
| **1:20** | **$1.6\pm0.1\times10^4$** | **---** | **−0.097** |

For Kaem:Zn(II) with varying ratios, the concentration of Kaem is fixed to be 100 μM.Oxidation potentials were relative to ferrocene for the actual solution used for $\beta$-Car$^{\bullet+}$ scavenging.

**3.3.2 DPPH• Radical Scavenging Kinetics.** The reaction between 2,2-diphenyl-1-picrylhydrazyl radical (DPPH•) and Kaem as well as the Zn(II)-kaempferol complexes were followed as changes in absorbance in ethanol by stopped-flow spectroscopy as shown in Figure 5. Upon addition of 100 μM Kaem to 100 μM DPPH• solution, the decay of absorbance at 516 nm is accelerated, while no effect is seen for addition of up to 1000 μM Zn(II). The rate of DPPH• scavenging for Kaem is strongly accelerated by addition of Zn(II).

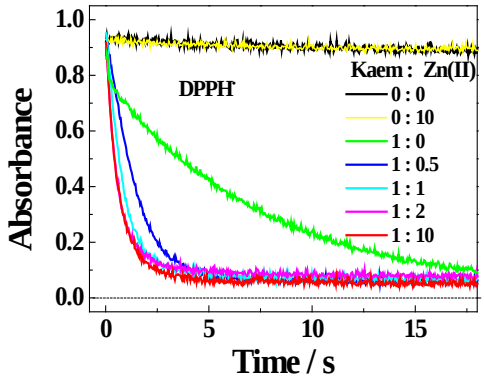


**Figure 5.** Absorbances at 516 nm for DPPH• scavenged by 100 μM Kaem, by 100 μM $Zn(CH_3COO)_2$, and by 100 μM Kaem with 50, 100, 200 and 1000 μM $Zn(CH_3COO)_2$ in ethanol at 25°C, respectively.

DPPH• radical scavenging is generally accepted as hydrogen atom transfer (HAT) mechanism.[50] Kaem, is in equilibrium with the 1:1 and 1:2 Zn(II)-kaempferol complexes in the ethanol solutions, and the reaction rate depends on three parallel reactions:

$$DPPH^{\bullet} + Kaem \xrightarrow{k_2^{Kaem}} DPPH\text{-}H + (Kaem{-}H)^{\bullet} \quad (10)$$

$$DPPH^{\bullet} + Zn(II)\text{-}(Kaem{-}H)_2 \xrightarrow{k_2^{Zn(II)\text{-}(Kaem\text{-}H)_2}} DPPH\text{-}H + Zn(II)\text{-}[(Kaem{-}H)_2\text{-}H]^{\bullet} \quad (11)$$

$$DPPH^{\bullet} + Zn(II)\text{-}(Kaem{-}2H) \xrightarrow{k_2^{Zn(II)\text{-}(Kaem\text{-}2H)}} DPPH\text{-}H + Zn(II)\text{-}[(Kaem{-}2H)\text{-}H]^{\bullet} \quad (12)$$

in which, $k_2^{Kaem}$, $k_2^{Zn(II)\text{-}(Kaem\text{-}H)_2}$ and $k_2^{Zn(II)\text{-}(Kaem\text{-}2H)}$ are second order rate constants for reactions of DPPH• with Kaem, Zn(II)-(Kaem−H)$_2$, and Zn(II)-(Kaem−2H), respectively. The changes in absorbance including the decay of DPPH• and formation of reaction product DPPH-H, could for all conditions be described as an exponential decay with an observed rate constant, $k_{DPPH^{\bullet}}$, within a 2 s time period:

$$A_{\text{DPPH}^\bullet} + A_{\text{DPPH-H}} = B \times e^{-k_{\text{DPPH}^\bullet} \cdot t} \quad (13)$$

$$\varepsilon_{\text{DPPH}^\bullet} \cdot c_{\text{DPPH}^\bullet} \cdot l + \varepsilon_{\text{DPPH-H}} c_{\text{DPPH-H}} l = B \times e^{-k_{\text{DPPH}^\bullet} \cdot t} \quad (14)$$

in which, $A_{\text{DPPH}^\bullet}$ and $A_{\text{DPPH-H}}$, $\varepsilon_{\text{DPPH}^\bullet}$ (9660 $\text{L}\cdot\text{mol}^{-1}\cdot\text{cm}^{-1}$)[51] and $\varepsilon_{\text{DPPH-H}}$, $c_{\text{DPPH}^\bullet}$ and $c_{\text{DPPH-H}}$ are absorbances, the extinction coefficients and concentrations of DPPH$^\bullet$ and the stable reaction product DPPH-H, respectively. *B* is pre-exponential factor. The extinction coefficient of DPPH-H is calculated to be $\varepsilon_{\text{DPPH-H}}$ =644 $\text{L}\cdot\text{mol}^{-1}\cdot\text{cm}^{-1}$, based on complete transformation of initial 100 μM ($10^{-4}$ M) DPPH$^\bullet$ to the stable reaction product DPPH-H ($c_{\text{DPPH-H}}=10^{-4}-c_{\text{DPPH}^\bullet}$). Reaction rate equation can be written as:

$$c_{\text{DPPH}^\bullet}(\varepsilon_{\text{DPPH}^\bullet} - \varepsilon_{\text{DPPH-H}}) = B \times e^{-k_{\text{DPPH}^\bullet} \cdot t} - 10^{-4} \times \varepsilon_{\text{DPPH-H}} \quad (15)$$

The initial reaction rates are calculated as:

$$rate_{t=0} = -\left.\frac{dc_{\text{DPPH}^\bullet}}{dt}\right|_{t=0} = \frac{B \times k_{\text{DPPH}^\bullet}}{\varepsilon_{\text{DPPH}^\bullet} - \varepsilon_{\text{DPPH-H}}} \quad (16)$$

Considering the reactions of equations (10-12), the initial reaction rate may also be written as:

$$-\left.\frac{dc_{\text{DPPH}^\bullet}}{dt}\right|_{t=0} = c^{t=0}_{\text{DPPH}^\bullet} \times \left(k_2^{\text{Kaem}} \times c^{t=0}_{\text{Kaem}} + k_2^{\text{Zn(II)-(Kaem-H)}_2} \times c^{t=0}_{\text{Zn(II)-(Kaem-H)}_2} + k_2^{\text{Zn(II)-(Kaem-2H)}} \times c^{t=0}_{\text{Zn(II)-(Kaem-2H)}}\right) \quad (17)$$

Individual second order rate constants, $k_2^{\text{Kaem}}$ =(1.59±0.01)×$10^3$ $\text{L}\cdot\text{mol}^{-1}\cdot\text{s}^{-1}$, $k_2^{\text{Zn(II)-(Kaem-H)}_2}$ =(1.30±0.07)×$10^4$ $\text{L}\cdot\text{mol}^{-1}\cdot\text{s}^{-1}$ and $k_2^{\text{Zn(II)-(Kaem-2H)}}$ =(2.48±0.03)×$10^4$ $\text{L}\cdot\text{mol}^{-1}\cdot\text{s}^{-1}$ are calculated from the distributions of Kaem, Zn(II)-(Kaem−H)$_2$ and Zn(II)-(Kaem−2H) (Table 1) at initial time (*t*=0 s) and the observed rate constant $k_{\text{DPPH}^\bullet}$ at varying Zn(II):Kaem ratios (Table 2). Zn(II)-(Kaem−H)$_2$ is found to be ~8 times as fast as the parent Kaem in DPPH$^\bullet$ scavenging, while Zn(II)-(Kaem−2H) is found to be ~16 times as fast as Kaem.

**3.4 Structural and Thermodynamic Analyses.** Molecular structures of Zn-kaempferol complexes and of Kaem for comparison were optimized using DFT method and are shown in Figure S5. H exa-coordinate structures of all Zn-kaempferol complexes are more stable than tetra-coordinated as indicated by imaginary frequencies found in frequency calculation for tetra-coordination.[52] In the optimized structures

of both 1:1 and 1:2 Zn(II)-kaempferol complexes, Zn(II) ion coordinate to oxygen atoms of Kaem. The other coordination sites in octahedron are occupied by solvent ethanol, not shown in Figure S5 for clarity. Zn(II) ion and 4 oxygen atoms in 1:2 Zn(II)-(Kaem−H)$_2$ are coplanar with $C_i$ point group symmetry. 4-O-Zn bonds in all Zn(II)-kaempferol complexes are longer than 3-O-Zn bonds due to stronger electron withdrawal effect of 4-carboxyl than 2,3-carbon-carbon double bond. Both 3- and 4-O-Zn bonds in 1:2 Zn(II)-(Kaem−H)$_2$ are longer than those in 1:1 Zn(II)-(Kaem−H)$^+$ and Zn(II)-(Kaem−2H) implicating stronger binding between oxygen and Zn(II) in 1:1 complexes. Two Kaem ligands simultaneously coordinated to Zn(II) together disperse the electronic density and weaken bond strength.

Thermodynamic parameters, including proton dissociation enthalpy (PDE), ionization potential (IP), bond dissociation energy (BDE) of Zn(II)-kaempferol complexes and of Kaem for comparison, were calculated and are listed in Table 3. Significant effects are seen for phenol acidity increase for 5, 7 and 4´-hydroxyls of Kaem in 1:1 Zn(II)-(Kaem−H)$^+$ through coordination to Zn(II) with the lowest PDE value (276.32~278.07 kcal·mol$^{-1}$), ~50 kcal·mol$^{-1}$ less than Zn(II)-(Kaem−H)$_2$ and Kaem with similar PDE values (326~328 kcal·mol$^{-1}$). 1:1 Zn(II)-(Kaem−H)$^+$ with much lower PDE values than Kaem is thus easy to lose the second proton (*the first from 3-hydroxyl by coordination with Zn(II)*) forming Zn(II)-(Kaem−2H), which is in good agreement with above experimental observations of 15 nm red-shift of Zn(II)-(Kaem−2H) relative to Zn(II)-(Kaem−H)$_2$ as seen in Figure 1a, 1c and 2. While the acidity of three phenols in Zn(II)-(Kaem−H)$_2$ remains almost unaffected by coordination with similar PDE values to phenols in Kaem. PDE values of three phenols (5, 7 and 4´) in Zn(II)-(Kaem−H)$^+$ are very close. 7-Hydroxyl has slightly lower PDE value than the other two, and 7-phenolate is accordingly used as the most dominating deprotonated forms of Zn(II)-(Kaem−2H) in Scheme 1, and in the following descriptions of BDE, IP as well as radical scavenging mechanism as shown in Scheme 2.

**Table 3.** Calculated bond lengths of $L_{O\text{-}Zn}$ (Å), proton dissociation energy(PDE), ionization potential (IP), and bond dissociation energy (BDE) of Kaem and Zn-kaempferol complexes in kcal·mol$^{-1}$.

| Compound | | Kaem | Zn(II)-(Kaem–H)$_2$ | Zn(II)-(Kaem–H)$^+$ | Zn(II)-(Kaem–2H) | |
|---|---|---|---|---|---|---|
| $L_{O\text{-}Zn}$ (Å) | 3-O-Zn | --- | 2.06 | 2.00 | 1.98 | |
| | 4-O-Zn | --- | 2.15 | 2.08 | 2.02 | |
| PDE (kcal·mol$^{-1}$) | 3-OH | 331.97 | | | | |
| | 5-OH | 337.27 | 333.63 | 278.07 | | |
| | 7-OH | 322.58 | 321.79 | 276.32 | | |
| | 4´-OH | 322.54 | 324.04 | 277.21 | | |
| IP (kcal·mol$^{-1}$) | | 167.02 | 140.32 | 199.62 | 5-O$^-$ | 122.26 |
| | | | | | 7-O$^-$ | 122.10 |
| | | | | | 4´-O$^-$ | 121.43 |
| BDE (kcal·mol$^{-1}$) | 3-OH | 78.12 | | | --- | --- |
| | 5-OH | 92.34 | 87.08 | 83.67 | 7-O$^-$ | 79.95 |
| | | | | | 4´-O$^-$ | 70.48 |
| | 7-OH | 83.46 | 78.45 | 83.54 | 5-O$^-$ | 76.72 |
| | | | | | 4´-O$^-$ | 66.46 |
| | 4´-OH | 77.76 | 73.91 | 78.99 | 5-O$^-$ | 68.15 |
| | | | | | 7-O$^-$ | 67.35 |

IP values in Table 3 show that, compared to parent Kaem, coordination of Kaem decreases IP of both Zn(II)-(Kaem−2H) and Zn(II)-(Kaem−H)$_2$, but not for Zn(II)-(Kaem−H)$^+$. Due to electron withdrawal by Zn(II) ion, coordination of the first Kaem to Zn(II) decreases PDE in Zn(II)-(Kaem−H)$^+$ and further decreases IP in Zn(II)-(Kaem−2H), but coordination of the second Kaem in Zn(II)-(Kaem−H)$_2$ more than outbalance this electron withdrawal effect, resulting in Zn(II)-(Kaem−H)$_2$ having a higher IP than Zn(II)-(Kaem−2H) but lower than Kaem. The IP of Zn(II)-(Kaem−2H) (~122 kcal·mol$^{-1}$), is far lower than that of Zn(II)-(Kaem−H)$_2$ (140.32 kcal·mol$^{-1}$), Kaem (167.02 kcal·mol$^{-1}$) and Zn(II)-(Kaem−H)$^+$ (199.62 kcal·mol$^{-1}$), in agreement with far lower oxidation potential –0.097 V than the potentials of ~0.170 V for both Zn(II)-(Kaem−H)$_2$ and Kaem. The lowest oxidation potential for Zn(II)-(Kaem−2H) agrees well with this complex being the only electron donor observed in $\beta$-Car$^{\bullet+}$ radical scavenging.

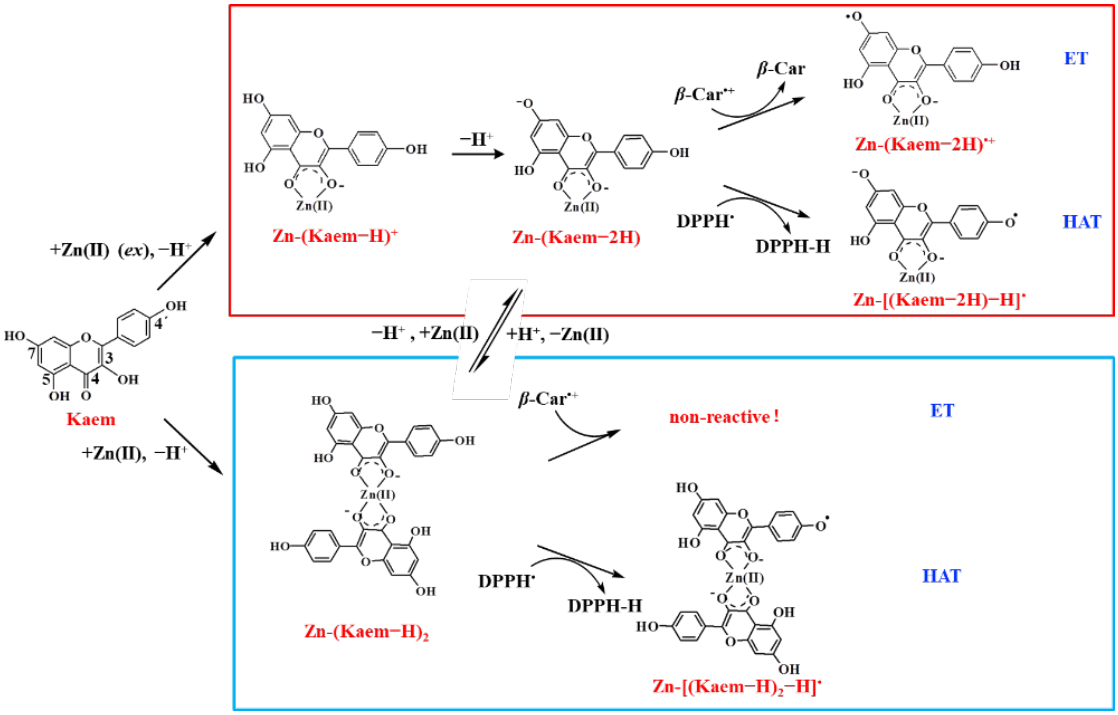


**Scheme 2.** Proposed mechanism of Kaem binding to Zn(II) and radical scavenging of Zn(II)-kaempferol complexes.

Zn(II)-(Kaem−2H) is also found having the lowest BDE among all Zn(II)-kaempferol complexes and Kaem. Although 7-hydroxyl for 4-deprotonation in Zn(II)-(Kaem−2H) has the lowest BDE, 66.46 kcal·mol$^{-1}$, 4′-hydroxyl for 7-deprotonation in Zn(II)-(Kaem−2H) with the second lowest BDE, 67.35 kcal·mol$^{-1}$, is believed to be the most dominating DPPH$^{\bullet}$ scavenging site due to 7-phenolate form being the dominating deprotonated form of Zn(II)-(Kaem−2H), as seen in Scheme 2. Similarly, the 4′-hydroxyl in 1:2 Zn(II)-(Kaem−H)$_2$ also has relatively lower BDE, 73.91 kcal·mol$^{-1}$, lower than parent Kaem, 77.76 kcal·mol$^{-1}$.[53] These results may explain 16 times for Zn(II)-(Kaem−2H) and 8 times for Zn(II)-(Kaem−H)$_2$, as fast as Kaem for scavenging rates in DPPH$^{\bullet}$ radical scavenging.

## 4. DISCUSSION

Flavonoids are among the most extensively investigated phytochemicals due to their diverse pharmacological and therapeutic activities. The ability of chelating with metal ions for flavonoids has brought about emergence of a new category of molecules with a broader spectrum of pharmacological activities. Flavonoid-based metal complexes are mostly found enhancement in antioxidant, anti-

inflammatory, anti-cancer activity and DNA binding with respect to their parent flavonoids.[54,55] Metal-flavonoid complexes are found sensitive to experimental conditions, i.e. concentration, pH, solvent, thus hampering acquirement of crystal structures, characterization of metal-flavonoid compounds and elucidation of molecular mechanism. S. Selvaraj et al. recently gave two proposed enhanced mechanism of metal-flavonoid complexes as antioxidants in scavenging reactive radicals. One is hydrogen abstraction by $DPPH^{\bullet}$ radical from an undissociated proton in phenolic hydroxyl chelating with metal ions. The other is metal ion as radical attacking site as SOD-mimic activity.[20] While, both two suggestions lack experimental evidences.

Kaempferol (Kaem), as a common flavonoid found in many vegetables and fruits, has been modified by coordination to metal ions, such as Zn(II), Eu(III), and Cu(II), etc.[10,56-59] Such metal-kaempferol complexes have been found having anticancer and DNA binding activities. In present study, upon addition Zn(II) to kaempferol, two zinc-kaempferol complexes with stoichiometries of 1:1 and 1:2 are formed, and characterized by IR, MS and $H^1$-NMR. Radical scavenging reactivities of two complexes towards the semi-stable radical $DPPH^{\bullet}$ and the highly reactive $\beta$-$Car^{\bullet+}$ are for the first time compared and determined in quantity based on molecular level.

Zn(II) was found to coordinate Kaem through the 3-hydroxyl and 4-carbonyl group with high affinity both for the first and for the second ligands. Spectral analyses and DFT calculations confirmed the first Kaem ligand coordination to Zn(II) significantly increase acidity of phenol in mono-coordinated complex $Zn\text{-}(Kaem\text{-}H)^+$ due to electron withdrawal effect Zn(II), thus easy to deprotonate forming 1:1 Zn-(Kaem-2H). Coordination of the second Kaem in $Zn(II)\text{-}(Kaem{-}H)_2$ balances this electron withdrawal effect, and deprotonation in phenolic group not occurred in $Zn(II)\text{-}(Kaem{-}H)_2$. Modification of Kaem in Zn(II)-(Kaem−2H), two proton leaving from each Kaem ligand, accordingly is more significant than that in $Zn(II)\text{-}(Kaem{-}H)_2$, one proton leaving from each Kaem ligand. Zn(II)-(Kaem-2H) and Zn(II)-

(Kaem−H)$_2$ transform into each other depending on the concentrations of Zn(II) and hydrogen ions, see equation (5).

Zn(II) is not redox active and Zn(II) coordination on kaempferol is accordingly not disturbed by change in the oxidation state of the metal[7]. The radical scavenging kinetics showed a clear pattern. Radical scavenging efficiencies for 1:1 and 1:2 complexes depend on types of complexes and reactive radicals, and reaction type. Zn(II)-(Kaem−2H) is the only scavenger for the very reactive $\beta$-Car$^{\bullet+}$ radical scavenging through ET mechanism, and also is the most efficient scavenger for the moderately reactive DPPH$^{\bullet}$ through HAT mechanism. While Kaem and with Zn(II)-(Kaem−H)$_2$ are non-reactive in $\beta$-Car$^{\bullet+}$ radical scavenging. Zn(II)-(Kaem−2H) reacts with DPPH$^{\bullet}$ 16 times and 2 times as fast as Kaem and Zn(II)-(Kaem−H)$_2$, respectively.

Radical scavenging results are in good agreement with DFT calculations. The IP of the deprotonated forms of Zn(II)-(Kaem−2H) is significantly smaller than of the protonated forms of Kaem and Zn(II)-(Kaem−H)$_2$, which notably have a large energy barrier for deprotonation. Accordingly, Zn(II)-(Kaem−2H) also has the lowest barrier for electron transfer to $\beta$-Car$^{\bullet+}$ as seen in laser photolysis. The BDE of 4´-OH hydroxyl were smallest among three unchelated phenolic hydroxyls in Kaem, Zn(II)-(Kaem−H)$_2$ and Zn(II)-(Kaem−2H) (*for 7-phenl deprotonation with the lowest PDE*), with the lowest value for Zn(II)-(Kaem−2H) and the highest value for Kaem. The most active scavenger of DPPH$^{\bullet}$ is accordingly concluded to be Zn(II)-(Kaem−2H), see Scheme 2.

The limited experimental studies on flavonoids partially are due to their poor water solubility. However, metal-flavonoid complexes are more hydrophilic and water-soluble than the corresponding ligands[19]. Such coordination in present study may occur spontaneously after intake of fruits and vegetables with flavonoids during digestion or may be in design of various kinds of metal-based drugs containing bioactive molecules of natural extraction. Structure-reactivity relationship obtained in this study, more efficient radical scavenging through increased phenol acidity in 1:1 Zn(II)-kaempferol complex than 1:2

Zn(II)-kaempferol complex and parent Kaem, may point toward a general mechanism for zinc as an antioxidant[1,2] and for increasing interest in the use of Zn(II) coordination complexes with low toxicity and low side effects in medicinal therapeutic applications[33].

## 5. CONCLUSIONS

Kaem binds to Zn(II) with high affinity entailing electron withdrawal from Kaem increasing phenolic acidity. Deprotonation of Kaem mono-coordinated to Zn(II) has a larger effect on electron donation than electron withdrawal by coordination to Zn(II). The 1:1 Zn(II)-kaempferol complex becomes more reducing than the uncoordinated Kaem and 1:2 Zn(II)-kaempferol complex. Phenolic acidity and oxidation potential are unaffected by coordination in the 1:2 Zn(II)-kaempferol complex compared to uncoordinated Kaem. Deprotonation, however, in general decrease ionization potential, and higher tendency of deprotonation for Kaem in Zn(II)-(Kaem−2H) than in Zn(II)-$(Kaem-H)_2$ fully outbalance the effect of electron withdrawal by coordination to Zn(II). The outbalance make Kaem in the 1:1 Zn(II) complex the very efficient radical scavenger.

**Supporting Information**.

S1. Reaction of Kaem and zinc(II), S2. Structural characterization of Zn(II)-kaempferol complexes. This material is available free of charge via the Internet at http://pubs.acs.org.

AUTHOR INFORMATION

**Corresponding Authors**

* rmhan@ruc.edu.cn

* ls@food.ku.dk

**Author Contributions**

The manuscript was written through contributions of all authors. / All authors have given approval to the final version of the manuscript.

**Notes**

The authors declare no competing financial interest.

**ACKNOWLEDGMENT**

This work has been supported by grants from Natural Science Foundation of China (Nos. 21573284 and 21673288).

**ABBREVIATIONS**

Kaem, kaempferol; DFT, density functional theory; *β*-Car, *β*-carotene; *β*-Car$^{\bullet+}$, *β*-carotene radical cation; CV, cyclic voltammetry; DPPH$^{\bullet}$, 2,2-diphenyl-1-picrylhydrazyl radical; PDE proton dissociation energy,; IP, ionization potential; BDE, bond dissociation energy.

**REFERENCES**

1. Lee, S. R. Critical role of zinc as either an antioxidant or a prooxidant in cellular systems. *Oxid. Med. Cell. Longev.* **2018**, *2018*, 1−11.

2. Maret, W. Zinc biochemistry: from a single zinc enzyme to a key element of life. *Adv. Nutr.* **2013**, *4*, 82−91.

3. Drewry, J. A.; Gunning, P. T. Recent advances in biosensory and medicinal therapeutic applications of zinc(II) and copper(II) coordination complexes. *Coord. Chem. Rev.* **2011**, *255*, 459−472.

4. Wilson, M.; Hogstrand, C.; Maret, W., Picomolar concentrations of free zinc(II) ions regulate receptor protein-tyrosine phosphatase *β* activity. *J. Biol. Chem.* **2012**, *287*, 9322-9326.

5. Tainer, J. A.; Getzoff, E. D.; Richardson, J. S.; Richardson, D. C. Structure and mechanism of copper, zinc superoxide dismutase. *Nature* **1983**, *306*, 284−287.

6. Prasad, A. S.; Bao, B.; Beck, F. W.; Kucuk, O.; Sarkar, F. H., Antioxidant effect of zinc in humans. *Free Radic. Biol. Med.* **2004**, *37*, 1182−1190.

7. Valko, M.; Morris, H.; Cronin, M. T. Metals, toxicity and oxidative stress. *Curr. Med. Chem.* **2005**, *12*, 1161−1208.

8. Bray, T. M.; Bettger, W. J. The physiological role of zinc as an antioxidant. *Free Radic. Biol. Med.* **1990**, *8*, 281−291.

9. Ikeda, N. E. A.; Novak, E. M.; Maria, D. A.; Velosa, A. S.; Pereira, R. M. S. Synthesis, characterization and biological evaluation of Rutin-zinc(II) flavonoid-metal complex. *Chem. Biol. Interact.* **2015**, *239*, 184−191.

10. Tu, L.-Y.; Pi, J.; Jin, H.; Cai, J.-Y.; Deng, S.-P. Synthesis, characterization and anticancer activity of kaempferol-zinc(II) complex. *Bioorg. Med. Chem. Lett.* **2016**, *26*, 2730−2734.

11. Sida-Arreola, J. P.; Sánchez, E.; Ojeda-Barrios, D. L.; Ávila-Quezada, G. D.; Flores-Córdova, M. A., J.; Márquez-Quiroz, C.; PreciadoRangel, P. Can biofortification of zinc improve the antioxidant capacity and nutritional quality of beans? *Emir. J. Food. Agric.* **2017**, *29*, 237−241.

12. Kellett, M. E.; Greenspan, P.; Pegg, R. B. Modification of the cellular antioxidant activity (CAA) assay to study phenolic antioxidants in a Caco-2 Cell Line. *Food Chem.* **2018**, *244*, 359-363.

13. Cren-Olivé, C.; Hapiot, P.; Pinson, J.; Rolando, C. Free radical chemistry of flavan-3-ols: Determination of thermodynamic parameters and of kinetic reactivity from short (ns) to long (ms) time scale. *J. Am. Chem. Soc.* **2002**, *124*, 14027−14038.

14. Liu, R.-H. Health-promoting components of fruits and vegetables in the diet. *Adv. Nutr.* **2013**, *4*, 384S−392S.

15. Chen, A. Y.; Chen, Y. C. A review of the dietary flavonoid, kaempferol on human health and cancer chemoprevention. *Food Chem.* **2013**, *138*, 2099−2107.

16. Puppo, A. Effect of flavonoids on hydroxyl radical formation by fenton-type reactions; influence of the iron chelator. *Phytochemistry* **1991,** *31*, 85−88.

17. Kasprzak, M. M.; Erxleben, A.; Ochocki, J. Properties and applications of flavonoid metal complexes. *RSC Adv.* **2015**, *5*, 45853−45877.

18. Qi, Y.; Jiang, M.; Cui, Y.-L.; Zhao, L.; Liu, S. Novel reduction of Cr(VI) from wastewater using a naturally derived microcapsule loaded with rutin-Cr(III) complex. *J. Hazard. Mater.* **2015**, *285*, 336−345.

19. Samsonowicz, M.; Regulska, E.; Kalinowska, M. Hydroxyflavone metal complexes-molecular structure, antioxidant activity and biological effects. *Chem.-Biol. Interact.* **2017**, *273*, 245−256.

20. Selvaraj, S.; Krishnaswamy, S.; Devashya, V.; Sethuraman, S.; Krishnan, U. M. Flavonoid-metal ion complexes: a novel class of therapeutic agents. *Med. Res. Rev.* **2014**, *34*, 677−702.

21. Raza, A.; Bano, S.; Xu, X.; Zhang, R. X.; Khalid, H.; Iqbal, F. M.; Xia, C.; Tang, J.; Ouyang, Z. Rutin-nickel complex: synthesis, characterization, antioxidant, DNA binding, and DNA cleavage activities. *Biol. Trace Elem. Res.* **2017,** *178*, 160−169.

22. Wang, H.-L.; Yang, Z.-Y.; Wang, B.-D. Synthesis, characterization and the antioxidative activity of copper(II), zinc(II) and nickel(II) complexes with naringenin. *Transit. Met. Chem.* **2006**, *31*, 470−474.

23. Yang, J.; Xu, Y.; Liu, H.-Y.; Han, R.-M.; Zhang, J.-P.; Skibsted, L. H. Genistein binding to copper(II)-solvent dependence and effects on radical scavenging. *Molecules* **2017,** *22*. 1757−1771.

24. Panhwar, Q. K.; Memon, S. Synthesis and evaluation of antioxidant and antibacterial properties of morin complexes. *J. Coord. Chem.* **2011,** *64*, 2117−2129.

25. Birjees Bukhari, S.; Memon, S.; Mahroof Tahir, M.; Bhanger, M. I. Synthesis, characterization and investigation of antioxidant activity of cobalt–quercetin complex. *J. Mol. Struct.* **2008**, *892*, 39−46.

26. Roy, S.; Mallick, S.; Chakraborty, T.; Ghosh, N.; Singh, A. K.; Manna, S.; Majumdar, S. Synthesis, characterisation and antioxidant activity of luteolin-vanadium(II) complex. *Food. Chem.* **2015**, *173*, 1172−1178.

27. Panhwar, Q. K.; Memon, S.; Bhanger, M. I. Synthesis, characterization, spectroscopic and antioxidation studies of Cu(II)–morin complex. *J. Mol. Struct.* **2010**, *967*, 47−53.

28. Samsonowicz, M.; Regulska, E. Spectroscopic study of molecular structure, antioxidant activity and biological effects of metal hydroxyflavonol complexes. *Free Radic. Biol. Med.* **2017**, *173*, 757−771.

29. Procházková, D.; Boušová, I.; Wilhelmová, N., Antioxidant and prooxidant properties of flavonoids. *Fitoterapia* **2011**, *82*, 513−523.

30. Moridani, M. Y.; Pourahmad, J.; Bui, H.; Siraki, A.; O'Brien, P. J. Dietary flavonoid iron complexes as cytoprotective superoxide radical scavengers. *Free Radic. Biol. Med.* **2003**, *34*, 243−253.

31. Barik, A.; Mishra, B.; Shen, L.; Mohan, H.; Kadam, R. M.; Dutta, S.; Zhang, H.-Y.; Priyadarsini, K. I. Evaluation of a new copper(II)-curcumin complex as superoxide dismutase mimic and its free radical reactions. *Free Radic. Biol. Med.* **2005**, *39*, 811−822.

32. Kim, E.-Y.; Pai, T.-K.; Han, O. Bioactive dietary polyphenols on zinc transport across the intestinal Caco-2 cell monolayers. *J. Agric. Food Chem.* **2011**, *59*, 3606-3612.

33. Mendiguchia, B. S.; Aiello, I.; Crispini, A. Zn(II) and Cu(II) complexes containing bioactive O,O-chelated ligands: Homoleptic and heteroleptic metal-based biomolecules. *Dalton Trans.* **2015**, *44*, 9321−9334.

34. Tesakova, M. V.; Semeikin, A. S.; Parfenyuk, V. I. Electrochemical determination of antioxidant properties of a series of tetraphenylporphyrin derivatives and their zinc complexes. *J. Porphyr. Phthalocya.* **2015**, *19*, 1−7.

35. de Souza, R. F.; De Giovani, W. F. Synthesis, spectral and electrochemical properties of Al(III) and Zn(II) complexes with flavonoids. *Spectrochim. Acta A* **2005**, *61*, 1985−1990.

36. Sulpizio, C.; Müller, S. T.; Zhang, Q.; Brecker, L.; Rompel, A. Synthesis, characterization, and antioxidant activity of $Zn^{2+}$ and $Cu^{2+}$ coordinated polyhydroxychalcone complexes. *Monatsh. Chem.* **2016**, *147*, 1871−1881.

37. Han, R.-M.; Chen, C.-H.; Tian, Y.-X.; Zhang, J.-P.; Skibsted, L. H. Fast regeneration of carotenoids from radical cations by isoflavonoid dianions: importance of the carotenoid keto group for electron transfer. *J. Phys. Chem. A* **2010**, *114*, 126−132.

38. Han, R.-M.; Tian, Y.-X.; Becker, E. M.; Andersen, M. L.; Zhang, J.-P.; Skibsted, L. H. Puerarin and conjugate bases as radical scavengers and antioxidants: molecular mechanism and synergism with beta-carotene. *J. Agric. Food. Chem.* **2007**, *55*, 2384−2391.

39. Frisch, M. J.; Trucks, G. W.; Schlegel, H. B.; Scuseria, G. E.; Robb, M. A.; Cheeseman, J. R.; Scalmani, G.; Barone, V.; Mennucci, B.; Petersson, G. A.; Nakatsuji, H.; Caricato, M.; Li, X.; Hratchian, H. P.; Izmaylov, A. F.; Bloino, J.; Zheng, G.; Sonnenberg, J. L.; Hada, M.; Ehara, M.;

Toyota, K.; Fukuda, R.; Hasegawa, J.; Ishida, M.; Nakajima, T.; Honda, Y.; Kitao, O.; Nakai, H.; Vreven, T.; Montgomery, Jr., J. A.; Peralta, J. E.; Ogliaro, F.; Bearpark, M.; Heyd, J. J.; Brothers, E.; Kudin, K. N.; Staroverov, V. N.; Kobayashi, R.; Normand, J.; Raghavachari, K.; Rendell, A.; Burant, J. C.; Iyengar, S. S.; Tomasi, J.; Cossi, M.; Rega, N.; Millam, J. M.; Klene, M.; Knox, J. E.; Cross, J. B.; Bakken, V.; Adamo, C.; Jaramillo, J.; Gomperts, R.; Stratmann, R. E.; Yazyev, O.; Austin, A. J.; Cammi, R.; Pomelli, C.; Ochterski, J. W.; Martin, R. L.; Morokuma, K.; Zakrzewski, V. G.; Voth, G. A.; Salvador, P.; Dannenberg, J. J.; Dapprich, S.; Daniels, A. D.; Farkas, Ö.; Foresman, J. B.; Ortiz, J. V.; Cioslowski, J.; Fox, D. J. Gaussian 09 Revision C.01.

40. Bartmess, J. E. Thermodynamics of the electron and the proton. *J. Phys. Chem.* **1994**, *98* , 6420−6424.

41. Ingham, K. C. On the application of Job's method of continuous variation to the stoichiometry of protein-ligand complexes. *Anal. Biochem.* **1975**, *68*, 660−663.

42. Vosburgh, W. C.; Cooper, G. R. Complex Ions. I. The identification of complex ions in solution by spectrophotometric measurements. *J. Am. Chem. Soc.* **1941**, *63*, 437−442.

43. Valente, J. V.; Buntine, M. A.; Lincoln, S. F., Ward, A. D. UV-Vis and fluorimetric $Al^{3+}$, $Zn^{2+}$, $Cd^{2+}$ and $Pb^{2+}$ complexation studies of two 3-hydroxyflavones and a 3-hydroxythioflavone. *Inorg. Chim. Acta* **2007**, *360*, 3380−3386.

44. Tan, J.; Wang, B.; Zhu, L. DNA binding and oxidative DNA damage induced by a quercetin copper(II) complex: potential mechanism of its antitumor properties. *J. Biol. Inorg. Chem.* **2009**, *14*, 727−739.

45. Uivarosi, V.; Badea, M.; Olar, R.; Draghici, C.; Barbuceanu, S. F. Synthesis and characterization of some new complexes of magnesium (II) and zinc (II) with the natural flavonoid primuletin. *Molecules* **2013**, *18*, 7631−7645.

46. Thangavel, P.; Viswanath, B.; Kim, S. Synthesis and characterization of kaempferol-based ruthenium (II) complex: A facile approach for superior anticancer application. *Mat. Sci. Eng. C* **2018**, *89*, 87−94.

47. Dar, R. A.; Naikoo, G. A.; Hassan, I. U.; Shaikh, A. M. Electrochemical behavior of kaempferol and its determination in presence of quercetin employing multi-walled carbon nanotube modified carbon paste electrode. *Anal. Chem. Res.* **2016**, *7*, 1−8.

48. Oztekin, Y.; Yazicigil, Z.; Ramanaviciene, A.; Ramanavicius, A. Polyphenol-modified glassy carbon electrodes for copper detection. *Sensor. Actuat. B: Chem.* **2011**, *152*, 37−48.

49. Kang, J.; Zhuo, L.; Lu, X.; Liu, H.; Zhang, M.; Wu, H. Electrochemical investigation on interaction between DNA with quercetin and Eu-Qu3 complex. *J. Inorg. Biochem.* **2004,** *98*, 79−86.

50. Shang, Y.-J.; Qian, Y.-P.; Liu, X.-D.; Dai, F.; Shang, X.-L.; Jia, W.-Q.; Liu, Q.; Fang, J.-G.; Zhou, B. Radical-scavenging activity and mechanism of resveratrol-oriented analogues: influence of the solvent, radical, and substitution. *J. Org. Chem.* **2009**, *74*, 5025−5031.

51. Butković, V.; Klasinc, L.; Bors, W. Kinetic study of flavonoid reactions with stable radicals. *J. Agric. Food Chem.* **2004,** *52*, 2816−2820.

52. Yasarawan, N.; Thipyapong, K.; Ruangpornvisuti, V. Chelation behavior of various flavonols and transfer of flavonol-chelated zinc(II) to alanylaspartic dipeptide: A PCM/DFT investigation. *J. Mol. Struct.* **2016**, *1107*, 278−290.

53. Chen, W.; Sun, S.; Cao, W.; Liang, Y.; Song, J., Antioxidant property of quercetin–Cr(III) complex: The role of Cr(III) ion. *J. Mol. Struct.* **2009,** *918*, 194−197.

54. Jabeen, E.; Janjua, N. K.; Hameed, S., *β*-Cyclodextrin assisted solubilization of Cu and Cr complexes of flavonoids in aqueous medium: A DNA-interaction study. *Spectrochim. Acta A Mol. Biomol. Spectrosc.* **2014**, *128*, 191−196.

55. Afanas'Eva, I. B.; Ostrakhovitch, E. A.; Mikhal'Chik, E. V.; Ibragimova, G. A.; Korkina, L. G., Enhancement of antioxidant and anti-inflammatory activities of bioflavonoid rutin by complexation with transition metals. *Biochem. Pharmacol.* **2001,** *61*, 677-684.

56. Zhang, G.; Guo, J.; Zhao, N.; Wang, J., Study of interaction between kaempferol–$Eu^{3+}$ complex and DNA with the use of the Neutral Red dye as a fluorescence probe. *Sensors. Actuat. B Chem.* **2010**, *144*, 239−246.

57. Cao, Y.; Wu, X.; Wang, M. Silver nanoparticles fluorescence enhancement effect for determination of nucleic acids with kaempferol–Al(III). *Talanta* **2011**, *84*, 1188−1194.

58. Marković, J. M. D.; Amić, D.; Lučić, B.; Marković, Z. S. Oxidation of kaempferol and its iron(III) complex by DPPH radicals: spectroscopic and theoretical study. *Monatsh. Chem.* **2014**, *145*, 557−563.

59. Avi, M. D. C. R.; García, A. Á. M.; Ureña, F. P. Electronic structure of kaempferol–$Cu^{2+}$ coordination compounds: a DFT, QTAIM and NBO study in the gas phase. *Theor. Chem. Acc.* **2015**, *134*, 52.181-190.

Table of Contents